Appendix 1

Ultrasound images were captured using diverse ultrasound diagnostic equipment, including Canon Aplio i900, Mindray R9, Mindray Resona 7, Siemens SC1000, Siemens SC2000, Philips EPIQ 5, Philips EPIQ 5g, Philips EPIQ 7C, GE LOGIQ E9, TOSHIBA Aplio 500, and SAMSUNG WS80A. The probe frequency was 7-10MHz. Patients assumed a supine position with their necks fully exposed, undergoing longitudinal and transverse multi-sectional neck scans.

Table S1 Pathological classification of 1,076 thyroid nodules

| Pathological classification	Training cohort (n=719)	Validation cohort (n=74)	Test cohort (n=283)
Benign nodules, n	411	8	175
Nodular goiter, n (%)	376 (91.5)	6 (75.0)	146 (83.4)
Adenoma, n (%)	18 (4.4)	0	8 (4.6)
Chronic lymphocytic thyroiditis, n (%)	12 (2.9)	2 (25.0)	20 (11.4)
Subacute thyroiditis, n (%)	5 (1.2)	0	1 (0.6)
Malignant nodules, n	308	66	108
Papillary thyroid carcinoma, n (%)	306 (99.4)	65 (98.5)	107 (99.1)
Medullary thyroid carcinoma, n (%)	2 (0.6)	1 (1.5)	1 (0.9)
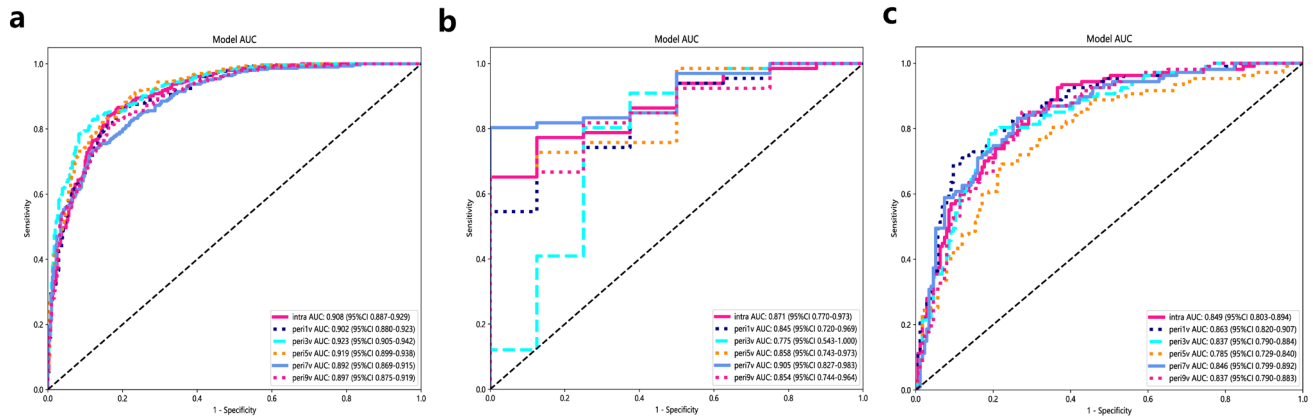
Figure S1 AUCs of intratumoral, intratumoral + peritumoral radiomics models in (A) training cohort, (B) validation cohort and (C) test cohort. AUC, area under the curve; CI, confidence interval; intra, intranodular; intra+p1, intranodular and perinodular with 1 pixel; intra+p3, intranodular and perinodular with 3pixels; intra+p5, intranodular and perinodular with 5 pixels; intra+p7, intranodular and perinodular with 7 pixels; intra+p9, intranodular and perinodular with 9 pixels.
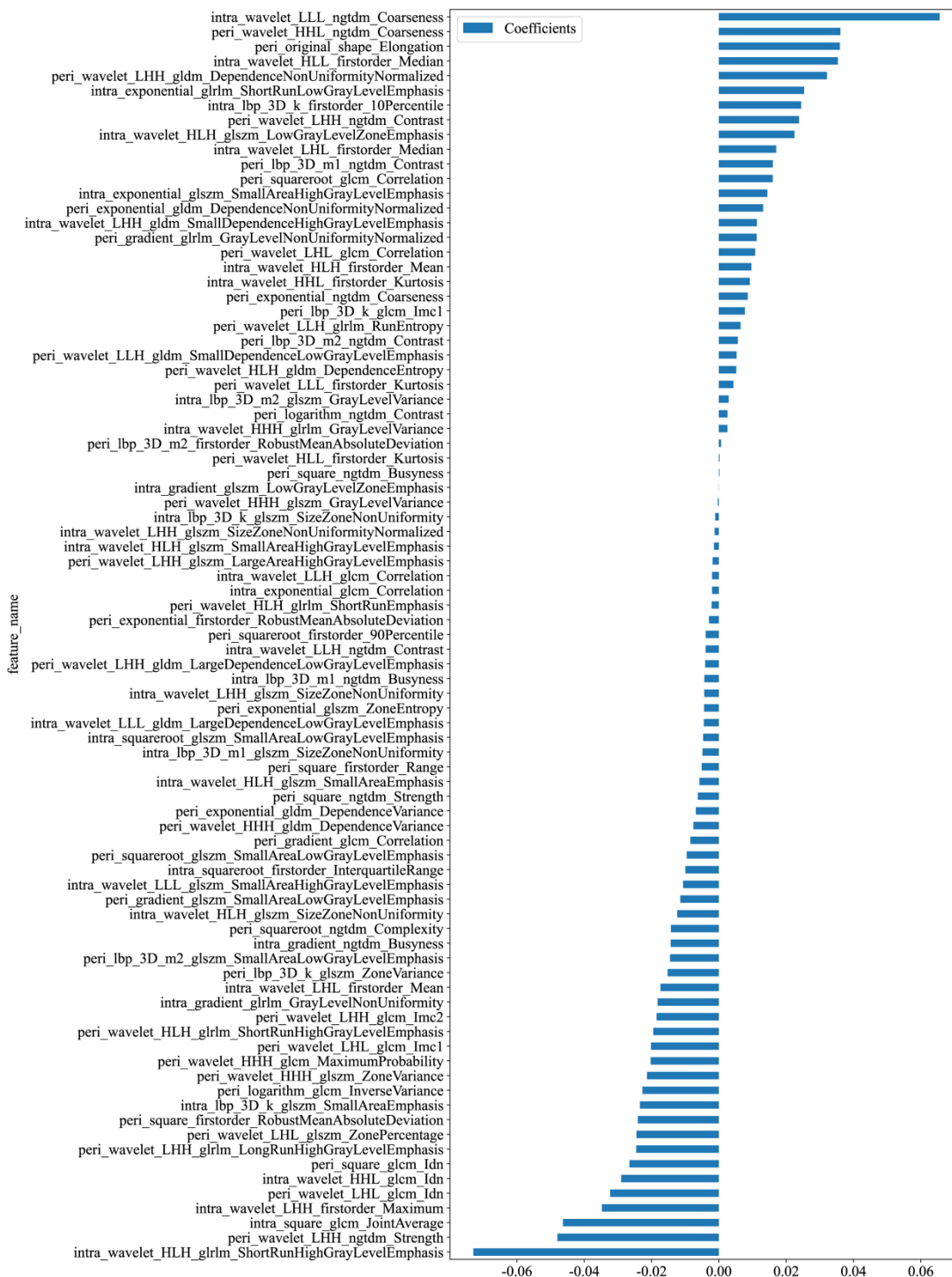
Figure S2 Detail radiomics features of Rad_Sig. Rad_Sig, radiomics signature.